Ferromagnetism, superconductivity and quantum criticality in uranium intermetallics

Nguyen Thanh, H.

Publication date
2008

8. Suppression of ferromagnetism and superconductivity in UCoGe doped with Si

8.1. Introduction

In the previous chapter, we have reported an extraordinary finding: the compound UCoGe is a new member of the small group of ferromagnetic superconductors. The small ordered moment and low Curie temperature locate UCoGe close to the ferromagnetic instability. The occurrence of superconductivity on the borderline of ferromagnetic order suggests UCoGe may present an example of triplet SC mediated by ferromagnetic spin-fluctuations. Using the Ehrenfest relation for second order phase transitions, we predicted that UCoGe is placed on the left side of the superconducting dome with respect to the critical point in the *p*-*T* phase diagram as illustrated in Fig. 7.13. It will to be very interesting to investigate the properties of UCoGe with respect to the proximity to a ferromagnetic quantum critical point (FM QCP) by applying mechanical pressure. However, such studies have not been performed yet.

In this chapter, we follow a different route and show that the magnetic instability in UCoGe can be approached by using chemical pressure, like reported for the suppression of magnetism in URhGe due to Ru doping in Chapter 4.

Suitable dopants for alloying UCoGe in search for the magnetic instability are Ru and Si. According to literature, among the neighboring TiNiSi isostructural U*TX* compounds only URuGe and UCoSi have a paramagnetic ground state [39,40,154]. The unit cell volume of URuGe is larger than that of UCoGe [39], and the electron configurations of Co (3*d* metal)

and Ru (4*d* metal) are different. Therefore, we expect that substitution on the Co site of Ru will lead to a rather complex hybridization changes, and the application of a negative chemical pressure. On the other hand, the unit cell volume of UCoSi is smaller than the one of UCoGe [39,40], and Ge and Si are isoeletronic. This indicates that in the case of substitution of Si on the Ge site the *f-d* hybridization associated with the magnetic order predominantly be influenced by the volume effect. We therefore decided to alloy UCoGe with Si in order to suppress ferromagnetism in UCoGe [183].

In this chapter, we report our investigation of the magnetic and transport properties of polycrystalline $UCoGe_{1-x}Si_x$ samples. The results show that ferromagnetism and superconductivity, which is confined to the FM phase, are both suppressed with increasing Si content and vanish at a critical concentration $x_{cr} \approx 0.12$. The observed NFL temperature dependence of the electrical resistivity and the smooth suppression of the ordered moment suggest a continuous FM QPT at x_{cr}. Similarly to $URh_{1-x}Ru_xGe$, these results open up an opportunity to investigate critical ferromagnetic spin-fluctuations of a ferromagnetic superconductor at ambient pressure.

8.2. Sample preparation and characterization

Polycrystalline $UCoGe_{1-x}Si_x$ samples with x in the range $0 \leq x \leq 0.20$ and $x = 1$ were prepared from nominal compositions $U_{1.02}Co_{1.02}$(Ge,Si) by arc-melting the constituents U (3N purity), Co (4N purity) and Ge, Si (5N purity) under a high-purity argon atmosphere. The weight loss was less than 0.1 %. The as-cast buttons were annealed for 10 days at 875 ^{o}C. The samples were cut by spark erosion in a bar-shape for the different experiments.

The EPMA analysis showed that the samples were homogeneous with 98 % of the sample volume forming the main matrix and about 2 % of secondary Uranium rich phases. The ratio between Ge and Si in our samples could not be determined exactly. In this chapter, the compositions of the $UCoGe_{1-x}Si_x$ samples are taken as the nominal compositions.

The lattice parameters of the $UCoGe_{1-x}Si_x$ alloys determined by X-ray powder diffraction are presented in Fig. 8.1. The *b* and *c* lattice parameters show a linear decrease, while the *a* parameter remains almost constant. The values obtained for the compounds UCoGe and UCoSi (a = 6.876 Å, b = 4.108 Å and c = 7.154 Å) are in good agreement with literature values [40]. Following Vegard's law, the unit cell volume Ω decreases linearly at a rate of

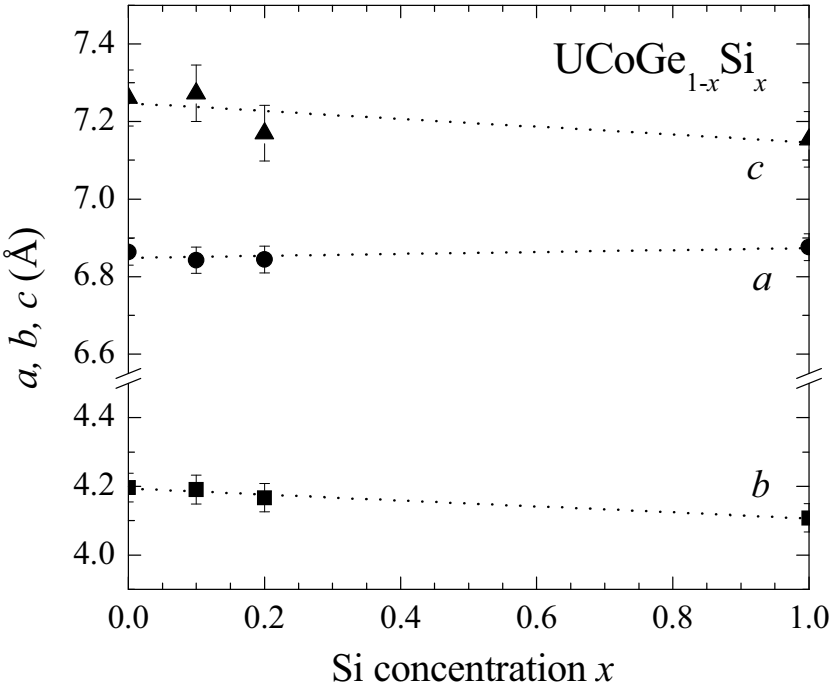

Figure 8.1 Lattice parameters of $UCoGe_{1-x}Si_x$ as a function of the Si concentration x measured at room temperature.

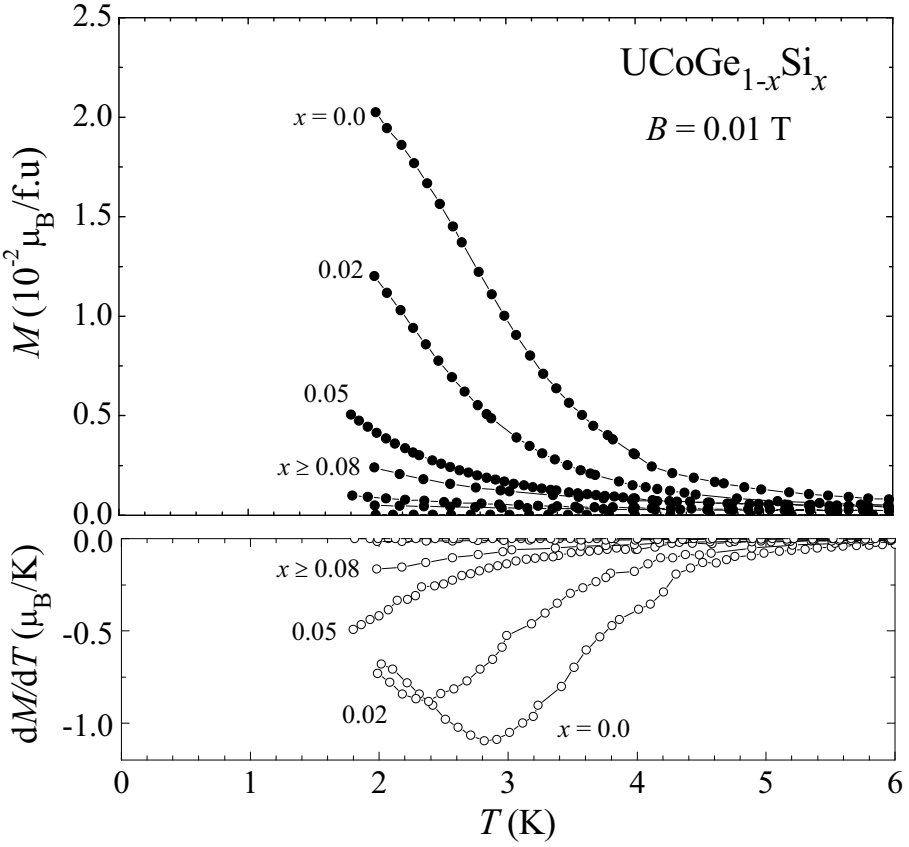

Figure 8.2 Upper frame: Temperature variation of the dc-magnetization measured in a field B = 0.01 T of $UCoGe_{1-x}Si_x$. For $x \geq 0.05$ the Curie temperature could not be determined from tha data. *Lower frame*: Temperature derivative of the magnetization.

0.059 Å^3/at.% Si.

The shortest Uranium-Uranium distance, $d_{U\text{-}U}$, calculated from the structural parameters, attains an almost constant value 3.47 ± 0.01 Å in the whole series.

8.3. Magnetic properties

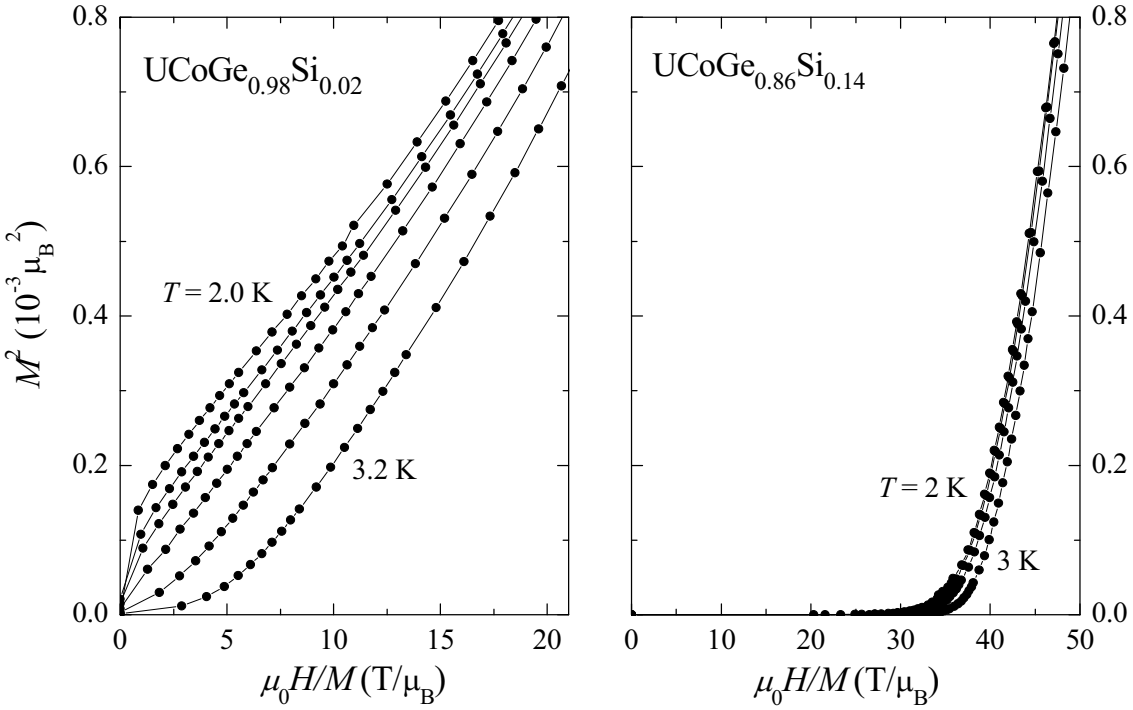

Figure 8.3 Arrott plots of the magnetization of $UCoGe_{1-x}Si_x$ alloys. *Left panel*: x = 0.02 with isotherms measured (from top to bottom) at T = 2.0, 2.2, 2.3, 2.5, 2.7 and 3.2 K. *Right panel*: x = 0.14 with isotherms measured (from top to bottom) at T = 2.0, 2.2, 2.5 and 3.0 K. The isotherm through the origin determines T_C = 2.5 K for x = 0.02. The ground state for x = 0.14 is paramagnetic.

The temperature variation of the magnetization $M(T)$ measured in a field of 0.01 T and its derivative $dM(T)/dT$ for the $UCoGe_{1-x}Si_x$ alloys are shown in Fig. 8.2. The magnetic order is monotonically suppressed upon Si doping. The Curie temperatures deduced from $(dM(T)/dT)_{min}$ agree well with those deduced from the Arrott plots (see Fig. 8.3). For x = 0 and 0.02 we find T_C = 3 and 2.5 K, respectively. For samples with $x \geq 0.05$, the ferromagnetic transition is not observed in the measured temperature interval above 2 K. The Arrott plots clearly indicate a paramagnetic ground state for x = 0.14.

In Fig. 8.4, the field dependence of the magnetization of the $UCoGe_{1-x}Si_x$ series measured in fields up to 5 T at 2 K is shown. The spontaneous moment M_S, extracted by fitting the

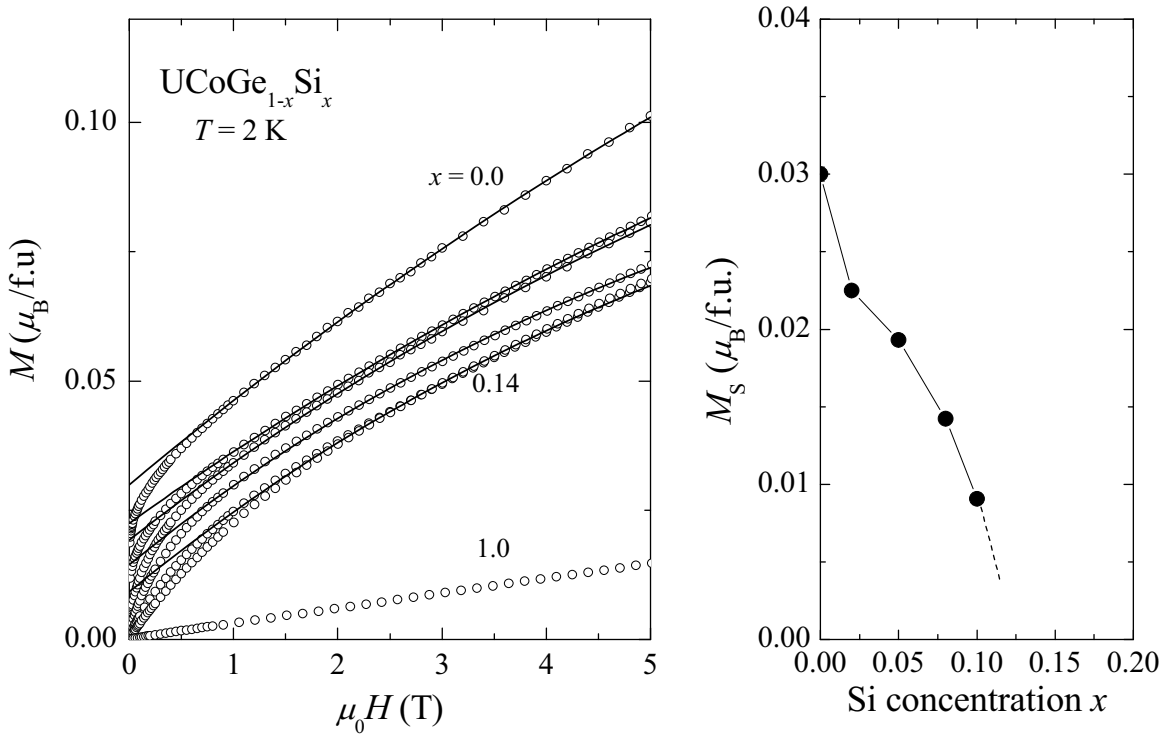

Figure 8.4 Left panel: Field dependence of the magnetization of $UCoGe_{1-x}Si_x$ alloys measured in a field up to 5 T at 2 K. The solid lines represent fits to Eq. 4.3 for the ordered compounds. Si concentrations are (from top to bottom) x = 0, 0.02, 0.05, 0.08, 0.1, 0.14 and 1. *Right panel*: The spontaneous moment M_S of $UCoGe_{1-x}Si_x$ as a function of Si concentration.

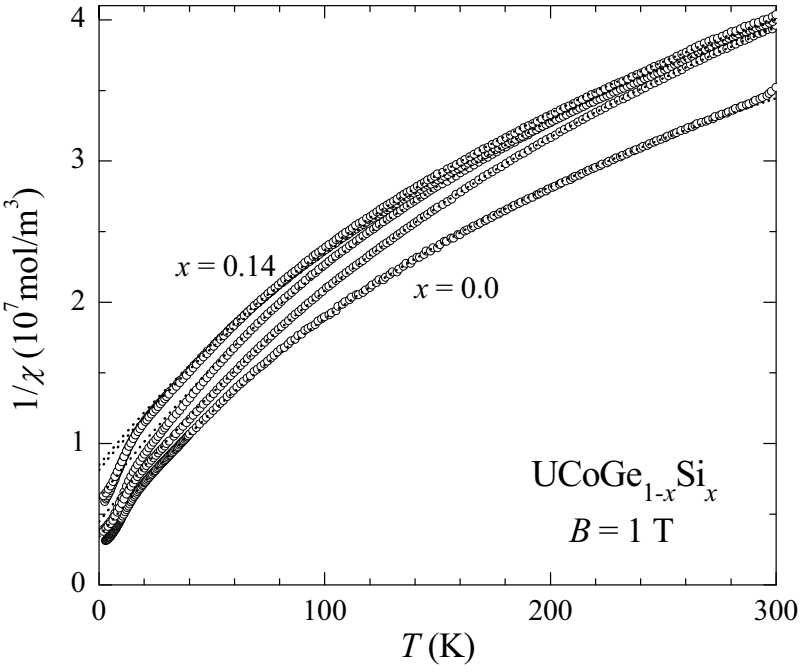

Figure 8.5 Temperature variation of the reciprocal susceptibility of $UCoGe_{1-x}Si_x$ alloys measured in a field of 1 T. The dotted lines are the best fits to the MCW law in the temperature range T = 50 - 300 K. Notice for x = 0.1 the data is plotted down to 50 mK.

experimental $M(H)$ data to Eq. 4.3, reduces with increasing Si content and smoothly goes to 0 in the concentration range $0.10 < x < 0.14$ (see the right panel of Fig. 8.4). This is a strong indication that the FM to paramagnetic transition as a function of x is a continuous phase transition.

The reciprocal susceptibility of $UCoGe_{1-x}Si_x$ measured in a field $B = 1$ T in the temperature range 2 - 300 K is shown in Fig. 8.5. The curves for various amounts of Si doping are similar, which indicate a weak variation with Si concentration. In the temperature range 50 - 300 K, the susceptibility can be well described by the MCW law with a temperature independent susceptibility $\chi_0 \sim 10^{-8}$ m^3/mol and an effective moment, $p_{eff} \sim 1.6 \pm 0.1$ μ_B/f.u. Some magnetization parameters of the series are listed in Table 8.1.

Table 8.1 The Curie temperature T_C and the parameters M_S, p_{eff} and θ of the $UCoGe_{1-x}Si_x$ alloys as deduced from the magnetization data.

x-Si	T_C (K)	M_S (μ_B/f.u.)	p_{eff} (μ_B/f.u.)	θ (K)
0	3.0	0.028	1.67	-15.7
0.02	2.5	0.023	1.60	-26.6
0.05	-	0.019	1.67	-20.8
0.1	-	0.009	1.60	-36.5
0.14	-	0.005	1.61	-38.7

8.4. Electrical resistivity

In Fig. 8.6, the temperature dependence of the electrical resistivity divided by the resistivity at room temperature ρ/ρ_{RT} of $UCoGe_{1-x}Si_x$ with x in the range $0 \le x \le 0.2$ is shown. Upon Si doping the residual resistivity values ρ_0 increase (see Table 8.2) and the residual resistance ratio RRR of 27 for $x = 0$ rapidly drops to a value of ~ 4 for $x \ge 0.1$. With increasing x the hump associated with the ferromagnetic transition shifts to lower temperature and becomes less pronounced.

As shown in Section 7.2.3 for pure UCoGe the resistivity is well described by the self consistent renormalization (SCR) theory for (clean) weak ferromagnets [82,158,159]. The theory predicts that the resisitivity due to spin fluctuations has a T^2- and $T^{5/3}$-dependence at temperatures below and above T_C, respectively. For doped $UCoGe_{1-x}Si_x$, the temperature

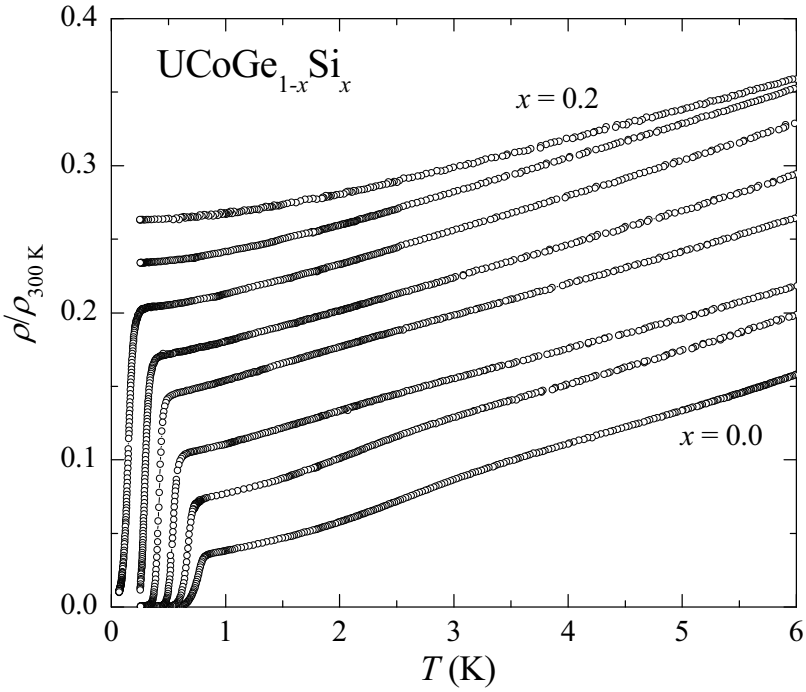

Figure 8.6 Temperature dependence of the electrical resistivity divided by the resistivity at room temperature ρ/ρ_{RT} of $UCoGe_{1-x}Si_x$ for $0 \leq x \leq 0.2$. Si concentrations are (from bottom to top) x = 0, 0.02, 0.04, 0.06, 0.08, 0.1, 0.14 and 0.2.

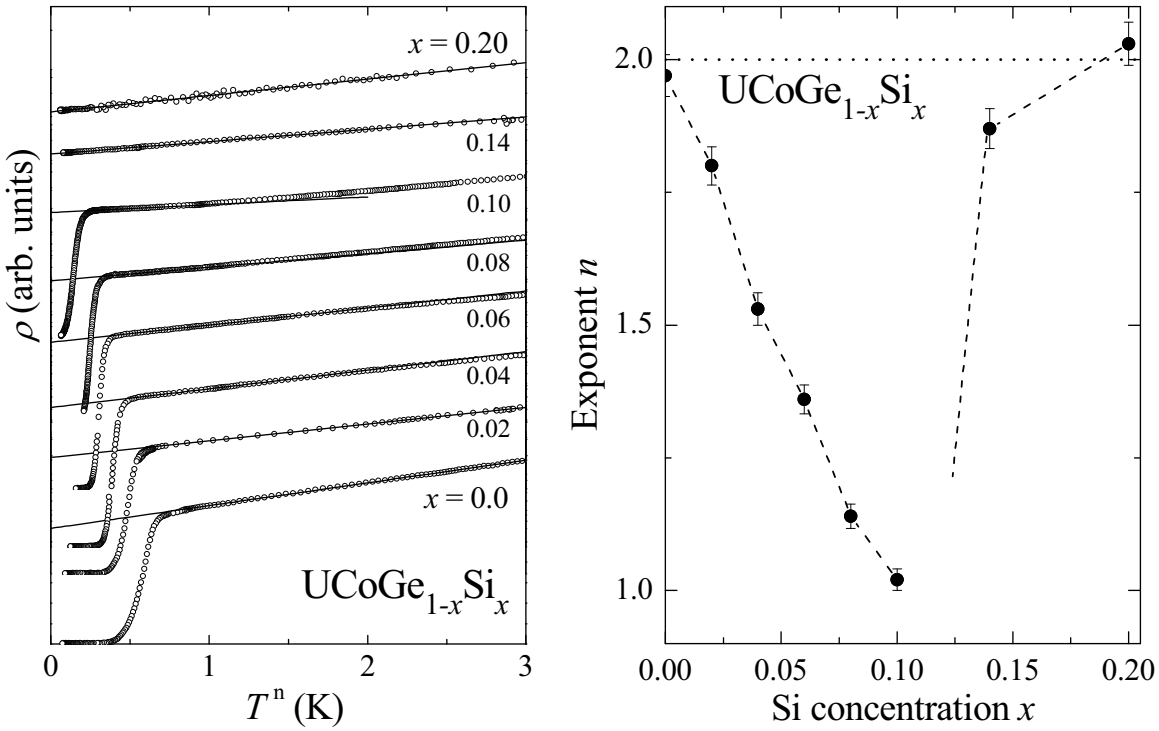

Figure 8.7 Left panel: The electrical resistivity ρ in arbitrary units of the $UCoGe_{1-x}Si_x$ alloys versus T^n. Si concentrations are (from bottom to top) x = 0, 0.02, 0.04, 0.06, 0.08, 0.1, 0.14 and 0.2. The solid lines represent the fits of the data to $\rho \sim T^n$. *Right panel*: The exponent n of the electrical resistivity of $UCoGe_{1-x}Si_x$ determined by $\rho \sim T^n$ versus Ru concentration. The horizontal dotted line indicates n = 2.

dependence of the resistivity is strongly influenced by disorder (*e.g.* as observed in the $URh_{1-x}Ru_xGe$ alloys). This hampers a discussion of the resistivity in terms of the SCR theory, and we restrict the analysis to fits of the data to $\rho = \rho_0 + AT^n$ for $T_S < T < T_C$. Upon Si doping, the value of the exponent n extracted by taking the best fit over the largest T interval (see Fig. 8.7) is reduced and attains a NFL value $n \approx 1$ for $x = 0.1$. Notice that close to the critical point the temperature range for the fit becomes very small and the value of n should be interpreted with care. At higher x, the exponent of the resistivity increases and reaches a value $n = 2$ for $x = 0.2$, which indicates the FL behavior is recovered.

Below 1 K, superconductivity is found (see Fig. 8.6), which coexists with FM. The resistive transition temperature T_S, which is defined as the mid-point of the resistivity drop is monotonically suppressed with Si substitution. For $x \geq 0.14$, SC is not observed anymore in the measurements down to 50 mK.

8.5. ac-susceptibility

Upon approaching the magnetic instability, the hump in the transport data associated with the ferromagnetic order of $UCoGe_{1-x}Si_x$ becomes less pronounced, while via the magnetization data, we could only determine the Curie temperature ($T > 2$ K) of samples with $x \leq 0.02$. Therefore, we used the ac-susceptibility technique to follow the magnetic ordering temperatures down to the mK regime.

Ac-susceptibility measurements have been carried out at a low frequency of 16 Hz and in a small driving field of $\sim 10^{-5}$ T. In Fig. 8.8, the temperature dependence of the ac-susceptibility of $UCoGe_{1-x}Si_x$ is presented. The maxima in χ_{ac} locate FM transitions. For pure UCoGe, the ordering peak is located at $T_C = 2.8$ K. This indicates T_C defined by χ_{ac} is somewhat smaller than the value deduced from the magnetization data. With increasing Si doping, the peak becomes weaker, broadens and gradually moves to lower temperatures, as shown in the inset of Fig. 8.8. The χ_{ac} measurements performed down to 50 mK show that FM order vanishes for $x \geq 0.14$.

The superconducting transition is observed as a rapid drop in χ_{ac} to a large diamagnetic value. For $x = 0$ the onset transition temperature in χ_{ac} $T_{S,onset}$ is 0.62 K. At this temperature the resistive transition is complete ($R = 0$). At the lowest temperature χ_{ac} reaches a value of 70% of the ideal screening value $\chi_S = -1/(1 - N)$ (here $N \approx 0.08$ is the demagnetizing factor

of our samples). Just like the FM order, superconductivity is progressively suppressed by replacing Ge by Si. For $x \geq 0.14$, we did not observe any sign of superconductivity for temperatures down to 50 mK.

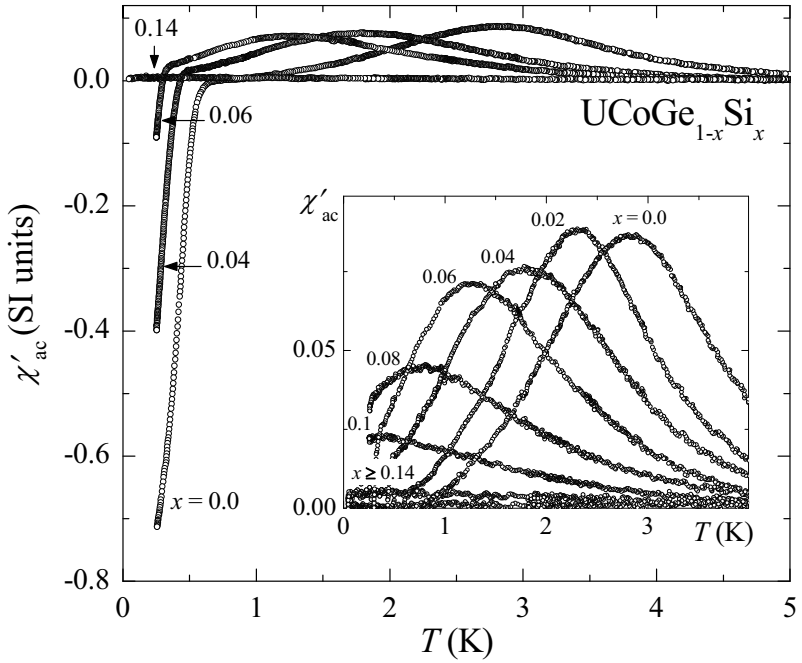

Figure 8.8 Temperature dependence of the ac-susceptibility of the $UCoGe_{1-x}Si_x$ alloys for x = 0.0, 0.04, 0.06 and 0.14. The inset shows ac-susceptibility around the FM transition for x in the range $0 \leq x \leq 0.2$.

Table 8.2 The critical temperatures T_C and T_S deduced from magnetization, transport and susceptibility data, and the parameters ρ_0, n and A obtained by fitting the resistivity to $\rho = \rho_0 + AT^n$ (Eq. 4.5) for $UCoGe_{1-x}Si_x$.

x-Si	T_C (K)		T_S (K)		ρ_0 (μΩcm)	n	A (μΩcm/K^n)
	$M(T)$	$\chi_{ac}(T)$	$\rho(T)$	$\chi_{ac}(T)$			
0	3.0	2.82	0.77	0.62	26	2	5.54
0.02	2.5	2.35	0.67	0.57	49	1.80	7.09
0.04	-	1.80	0.54	0.46	77	1.53	10.24
0.06	-	1.27	0.42	0.33	110	1.36	12.83
0.08	-	0.77	0.29	-	119	1.14	11.45
0.1	-	0.37	0.15	-	214	1.02	12.78
0.14	-	-	-	-	154	1.87	5.22
0.2	-	-	-	-	193	2	3.48

8.6. Discussion

8.6.1. *T-x* phase diagram

From the $M(T)$, $\rho(T)$ and $\chi_{ac}(T)$ data presented above, we construct a temperature-composition phase diagram $T_{C,S}(x)$ for $UCoGe_{1-x}Si_x$, as given in Fig. 8.9. With increasing Si doping, both the Curie temperature and the superconducting transition temperature are monotonically reduced to zero. T_C is suppressed quasi-linearly, at least till $x = 0.08$, at a rate $dT_C/dx = -0.25$ K/at.%Si. By extrapolating $T_C(x) \rightarrow 0$ we arrive at a critical Si concentration for the suppression of FM order $x_{cr} = 0.11$. While a tail in $T_C(x)$ appears for $x > 0.08$. T_S, determined resistively by the midpoint of the resistive transition, is suppressed somewhat faster than linear, initially at a rate $dT_S/dx = -0.06$ K/at.%Si. The $T_S(x)$ values measured by $\chi_{ac}(T)$ for $x \leq 0.06$, signal the onset bulk SC and follow the same trend. For $x \geq 0.14$ where the magnetism is completely suppressed, we did not observe any sign of the SC state in the samples. Thus we conclude superconductivity is confined to the ferromagnetic state. By making a smooth extrapolation of the phase lines, we obtain a critical concentration for Si doping $x_{cr} \approx 0.12$ at which both SC and FM order vanish.

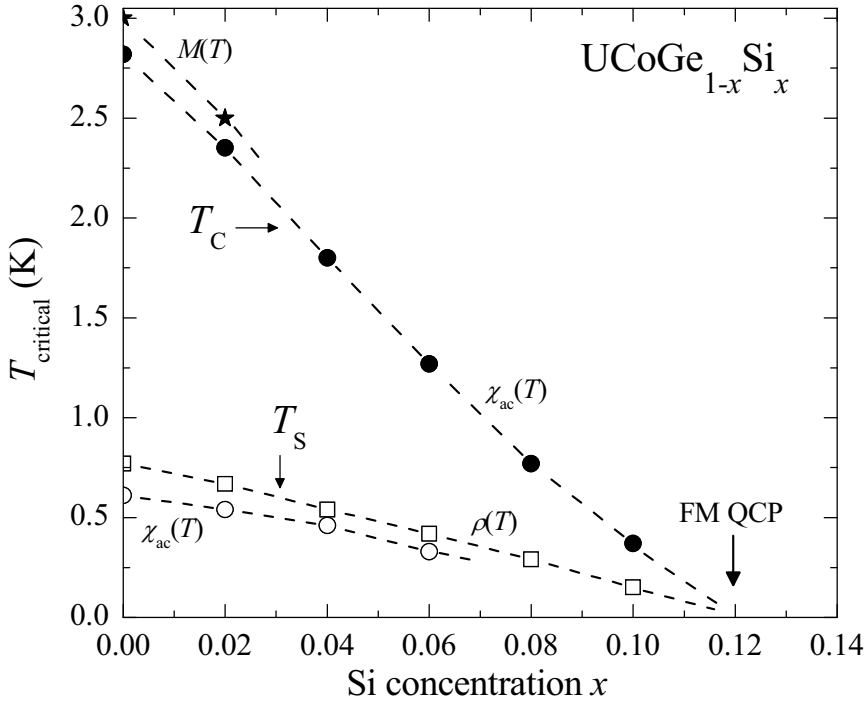

Figure 8.9 Temperature-composition phase diagram $T(x)$ of $UCoGe_{1-x}Si_x$. The Curie temperature T_C and the superconducting transition temperature T_S are determined from $M(T)$, $\rho(T)$ and $\chi_{ac}(T)$. The dashed lines serve to guide the eye.

8.6.2. Hybridization phenomena

In order to compare the volume effects due to Si alloying and hydrostatic pressure, we take a value for the isothermal compressibility $\kappa = -V^{-1}(dV/dp)$ of 0.8 $Mbar^{-1}$ [121]. A simple calculation shows that 1 at.% Si corresponds to a chemical pressure of 0.34 kbar. As mentioned in Chapter 7, for pure UCoGe the calculation based on the Ehrenfest relation for second order phase transitions predicts that upon applying pressure T_C is reduced at the rate of -0.25 K/kbar, whereas T_S increases at a rate of ~ 0.023 K/kbar. Using these values we estimate a decrease of T_C of -0.085 K and an increase of T_S of 0.0078 K per at.% Si. These calculated values differ from the values deduced from the experimental data (dT_C/dx = -0.254 K/at.%Si, dT_S/dx = -0.067 K/at.%Si), which show that T_C is suppressed three times faster and that T_S gradually decreases with Si content. As regards superconductivity, clearly adding impurities strongly reduces T_S, which largely compensates the effect of the chemical pressure.

Similar to the case of URhGe doped with Ru, Co or Si, the evolution of magnetism in the $UCoGe_{1-x}Si_x$ alloys can be explained by the Doniach picture [28] or LMTO band-structure calculations [142] in which the strength of the long-range magnetic order is connected to the strength of the *f-d* hybridization. Upon doping the smaller Si atoms the 5*f*-3*d* hybridization strength increases, ferromagnetic order is reduced and vanishes at $x_{cr} \approx 0.12$. The critical behavior in the resistivity and magnetization data provide evidence for a continuous FM QPT, as observed in $URh_{1-x}Ru_xGe$ [184]. Near the critical concentration x_{cr}, the exponent n of the resistivity reduces to a minimum value of ~ 1 which is much smaller than the value n = 5/3 predicted for a FM QCP [80-82]. This is attributed to the disorder in the doped samples. For $x > x_{cr}$ the exponent n recovers the FL value of 2. Correspondingly, the ordered moment M_S smoothly decreases and goes to 0 near x_{cr}.

However, additional investigations, like specific heat studies, are needed in order to put the evidence for a FM QCP at $x_{cr} \simeq 0.12$ on a firm footing.

8.6.3. Dependence of superconductivity on disorder

In the above, we have presented evidence that the SC state is always contained within the FM phase. This is in accordance with a scenario of SC mediated by ferromagnetic spin-fluctuations [105,109,185,186]. On the other hand, T_S of unconventional superconductors is extremely impurity sensitive, not only to magnetic impurities but also to non-magnetic

impurities. In the case of UCoGe, replacing Ge by Si is like introducing non-magnetic impurities in a triplet superconductor. Consequently, SC is destroyed due to pair-breaking effects. However, the defect-driven suppression of T_S is partly compensated by T_S increasing due to chemical pressure. Also, one may speculate that upon approaching of the FM QCP, FM fluctuations stimulate triplet SC even more effectively stronger. Obviously, more experiments are needed to unravel the different pairing and de-pairing contributions to T_S in this system.

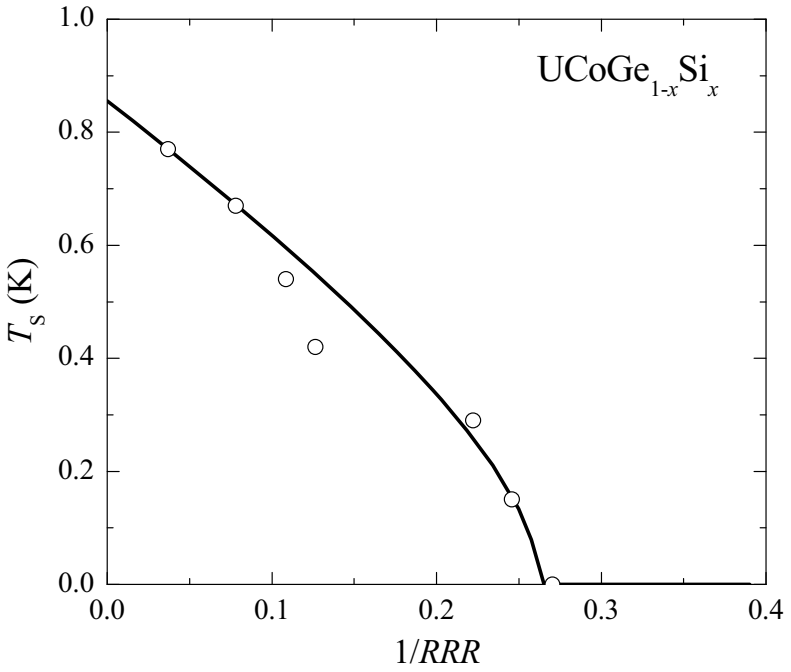

Figure 8.10 The superconducting transition temperature T_S as a function of 1/*RRR* of the $UCoGe_{1-x}Si_x$ alloys. The solid line is a fit of the data to the Abrikosov-Gor'kov pair-breaking function shown in Eq. 8.1 (for details see text).

Using a generalized form of the Abrikosov-Gor'kov (AG) theory [187] for the case of non-magnetic-impurities in unconventional superconductors, we can model the suppression of T_S as a function of doping level with an implicit relation for T_S [168,188-190].

$$\ln\left(\frac{T_{S0}}{T_S}\right) = \Psi\left(\frac{1}{2}+\frac{\alpha T_{S0}}{2\pi T_S}\right) - \Psi\left(\frac{1}{2}\right) \qquad (8.1)$$

where Ψ is the digamma function, T_{S0} is the superconducting transition temperature of the superconductor in the absence of impurities, and $\alpha = \hbar/2\tau\, k_B T_{S0}$ is the pair-breaking parameter with τ the lifetime due to elastic (nonmagnetic) potential scattering. Often α is taken to be proportional to ρ_0 or 1/*RRR*. (A recent example is provided by the defect-driven

suppression of *p*-wave SC in the paramagnet Sr_2RuO_4 [190].)

In Fig. 8.10, we show the suppression of T_S of the $UCoGe_{1-x}Si_x$ series as a function of 1/*RRR*, rather than the doping level. The data compare well with the generalized AG theory (Eq. 8.1) where we used $\alpha = 3.3/RRR$ as the best-fit parameter. This provides additional proof for an unconventional superconducting state in $UCoGe_{1-x}Si_x$. The detailed analysis of the variation of T_S due to Si doping can be found in Ref.[183].

In conclusion, we have investigated the suppression of ferromagnetism and superconductivity in polycrystalline UCoGe doped with Si via magnetization, transport and ac-susceptibility measurements. Both SC and FM order are depressed upon Si doping and vanish at the same critical concentration $x_{cr} \approx 0.12$. The SC phase is confined to the magnetic phase in accordance with a scenario of superconductivity mediated by critical FM fluctuations. The critical behavior in magnetization and transport data suggest a continuous FM QPT at x_{cr}. Further studies (*i.e.* specific heat measurement) are needed carried out in order to clarify this point. Nevertheless, these results offer a unique route to investigate the emergence of superconductivity near a FM QCP at ambient pressure.